bioRxiv preprint first posted online Jan. 29, 2020; doi: http://dx.doi.org/10.1101/2020.01.28.923748. The copyright holder for this preprint (which was not peer-reviewed) is the author/funder, who has granted bioRxiv a license to display the preprint in perpetuity. It is made available under a CC-BY-NC-ND 4.0 International license.

Encoding Innately Recognized Odors via a Generalized Population Code

Qiang Qiu[1], Yunming Wu[1], Limei Ma[1] and C. Ron Yu[1, 2, †]

[1]Stowers Institute for Medical Research, 1000 East 50th Street, Kansas City, MO 64110

[2]Department of Anatomy and Cell Biology, University of Kansas Medical Center, 3901 Rainbow Boulevard, Kansas City, KS 66160

[†]Correspondence: 816-926-4334 (office)

cry@stowers.org

bioRxiv preprint first posted online Jan. 29, 2020; doi: http://dx.doi.org/10.1101/2020.01.28.923748. The copyright holder for this preprint (which was not peer-reviewed) is the author/funder, who has granted bioRxiv a license to display the preprint in perpetuity. It is made available under a CC-BY-NC-ND 4.0 International license.

Abstract

Odors carrying intrinsic values often trigger instinctive aversive or attractive responses. Innate valence is thought to be conveyed through hardwired circuits along the olfactory pathway, insulated from influences of other odors. Here we show that in mice, mixing of innately aversive or attractive odors with a neutral odor abolishes the behavioral responses. Surprisingly, mixing of two odors with the same valence also abolishes the expected responses. Recordings from the olfactory bulb indicate that odors are not masked at the level of peripheral activation and glomeruli independently encode components in the mixture. However, crosstalk among the mitral/tufted cells changes their patterns of activity such that those elicited by the congruent mixtures can no longer be decoded as separate components. The changes in behavioral and mitral/tufted cell responses are associated with reduced activation of brain areas linked to odor preferences. Thus, interactions of odor channels at the earliest processing stage in the olfactory pathway lead to re-coding of odor identity. These results are inconsistent with insulated labeled lines and support a model of a common mechanism of odor recognition for both innate and learned valence associations.

bioRxiv preprint first posted online Jan. 29, 2020; doi: http://dx.doi.org/10.1101/2020.01.28.923748. The copyright holder for this preprint (which was not peer-reviewed) is the author/funder, who has granted bioRxiv a license to display the preprint in perpetuity. It is made available under a CC-BY-NC-ND 4.0 International license.

Introduction

Smell is a powerful sense in driving emotional reactions. For most animals, ethologically relevant odors often have innately associated values that signal danger or reward. Mice are attracted to food and urine of their own species, but they avoid scents from predators and odors associated with rotten food and decomposing carcasses. For example, 2-methyl butyric acid (2-MBA), found in spoiled food, 2,3,5-trimethyl-3-thiazoline (TMT) from fox feces, and 2-phenylethylamine (PEA) from bobcat urine can directly elicit avoidance behaviors [1-5]. The ability to properly recognize and respond to these odors is essential for survival of the animals in the wild.

The innateness and the consistency of the response among different individuals suggest that inborn pathways transmit the information of these odors to evoke stereotypical behaviors. In nematodes and insect species, this information appears to be transmitted through labeled line circuits [6]. In the mammalian brain, valence about aversive odors is also thought to be transmitted through dedicated pathways that bypass complex processing and link receptor activation directly to brain centers to elicit behavioral responses [7]. For example, PEA can activate the trace amine receptor TAAR4 [8]. Knock out of TAAR4 abolishes aversive response to PEA at low concentrations, suggesting information about PEA may pass through a highly specific pathway [3]. A variant of the hypothesis is that odor valence is topographically encoded, i.e., it is associated with specific regions of the olfactory bulb and in the brain [1,9]. For example, TMT or 2-MBA preferentially activate the dorsal olfactory bulb, which project to the posterolateral

bioRxiv preprint first posted online Jan. 29, 2020; doi: http://dx.doi.org/10.1101/2020.01.28.923748. The copyright holder for this preprint (which was not peer-reviewed) is the author/funder, who has granted bioRxiv a license to display the preprint in perpetuity. It is made available under a CC-BY-NC-ND 4.0 International license.

cortical amygdaloid area (PLCo) [1,10]. Genetic ablation of the dorsal olfactory bulb abolishes innate aversive responses to odors without affecting the recognition of the same odors in general [1].

In either case, innately recognized odors are expected to be encoded differently and separately from odors at large in two distinctive manners. First, the circuitry connecting the receptor neurons and brain centers that determine behavioral output is expected to be genetically hardwired and highly specific. While all neural circuits require genetic specification to some extent, the innate circuits are thought to be insensitive to environmental circumstances. Second, the pathways transmitting this information are expected to be insulated from background. Neural responses triggered by the innately recognized odor along the olfactory pathway are not expected to be altered by the presence of other odors. This is intuitive because animals exhibit aversive behavior towards the same compounds in different odor environments.

However, this view is being challenged by recent studies. In areas traditionally thought to encode odor valence, like the PLCo, a distributed representation for odors similar to that in the piriform cortex, and no apparent bias for the aversive odors are found [11]. Our recent study shows that development of innate odor preference is subject to changes by spontaneous neural activities and exposure to the odors during early development [12]. These studies suggest a more flexible mechanism in specifying these highly stereotyped circuits. In this study, we examine how the innately recognized odors trigger behavioral responses in the context of other odors. We show that interactions among mitral/tufted

bioRxiv preprint first posted online Jan. 29, 2020; doi: http://dx.doi.org/10.1101/2020.01.28.923748. The copyright holder for this preprint (which was not peer-reviewed) is the author/funder, who has granted bioRxiv a license to display the preprint in perpetuity. It is made available under a CC-BY-NC-ND 4.0 International license.

cells alter their representations of odors, the activation of brain regions associated with innate perception and behavioral responses. These results provide compelling evidence for a model of innate odor coding using a generalized population code that is similar to those for learned odor preference.

Results

Odor mixing abolishes innate valence

In an odor-seeking assay, an animal's approach toward the odor source is determined by at least three factors: novelty seeking, preference and odor habituation. For an attractive odor, prolonged investigation reflects attraction and novelty seeking. In contrast, an aversive odor may induce both novelty-seeking (for risk assessment) and avoidance. Odor preference is often assessed using place preference by associating odors with their spatial locations. However, intrinsic bias in spatial preference and scent marking can confound the readout [13,14]. To avoid intrinsic place bias, we have devised a computerized setup, PROBES, to perform automated single-chamber odor preference assays [13]. This setup provides an efficient and robust readout of the sampling of a single odor port in the habituation/dishabituation test (Fig. 1a). Using odors known to be attractive, neutral or aversive to mice, we examined odor investigation during first and second odor exposures after a period of habituation to clean air. The first exposure to mouse urines and peanut butter elicited vigorous investigation of the odor port, at a much higher level when

bioRxiv preprint first posted online Jan. 29, 2020; doi: http://dx.doi.org/10.1101/2020.01.28.923748. The copyright holder for this preprint (which was not peer-reviewed) is the author/funder, who has granted bioRxiv a license to display the preprint in perpetuity. It is made available under a CC-BY-NC-ND 4.0 International license.

compared with neutral and aversive odors (Fig. 1b, d). We therefore use the difference in investigation time between first odor and last air applications to index odor attraction (Fig. 1a, d). Investigations of the aversive odors such as coyote urine, 2-MBA, PEA or isoamylamine (IAMM) were considerably less than those of neutral odors but similar to that of air (Fig. 1c, e). When the mice were expose to the aversive odors a second time, investigation dropped significantly to below background level. The mice appeared to have avoided the odor port as exhibited by additional investigation once the odor delivery was stopped (Fig. 1c). We reasoned that investigation during the first exposure likely reflected the effect of two competing drives: avoidance and risk assessment (investigation). During the second exposure, aversion likely became the dominant drive resulting in a decrease in investigation. We therefore used the difference between the last air exposure and the second odor exposure to measure aversion (Fig. 1a, e).

We performed experiments using mixtures composed of equal parts of a neutral odor and an odor with innate valence (Fig. 1f-j). Whereas PEA alone caused pronounced avoidance and 2-hexanone (HXO) did not, mixing PEA with HXO elicited no aversive response (Fig. 1g). In the case of 2-MBA (aversive) and eugenol (EUG, neutral), the mixture even produced a slight preference (Fig. 1h). Similar observations were made for attractive odors. Both male and female urine samples were attractive to mice of the opposite sex, but maple odor was not (Fig. 1i). However, when maple was well mixed with the urine samples, the mixtures elicited little to no attraction (Fig. 1i, j). In all pairs tested, odor preferences were abolished when innately recognized odors were mixed with neutral odors.

bioRxiv preprint first posted online Jan. 29, 2020; doi: http://dx.doi.org/10.1101/2020.01.28.923748. The copyright holder for this preprint (which was not peer-reviewed) is the author/funder, who has granted bioRxiv a license to display the preprint in perpetuity. It is made available under a CC-BY-NC-ND 4.0 International license.

Mixing aversive odors abolishes behavioral avoidance

How might mixing abolish innate odor preference? One possible scenario is that the presence of a neutral odor could overpower the aversive odor and mask its presence. Alternatively, the two odors may activate separate brain regions that drive competing behaviors, resulting in nullification of aversive responses. In both scenarios, if we mixed two odors of the same valence, the mixture is expected to elicit the same behavioral responses. We, therefore, performed odor preference tests using mixtures of PEA with 2-MBA, and of PEA with IAMM (Fig. 1k, l). Strikingly, in both experiments, the mixtures did not elicit aversion. Similarly, well-mixed, innately attractive odors also reduced their attractiveness (Fig. 1m, n).

Linear decoding of odors from glomeruli responses

These behavioral experiment results were inconsistent with the labeled line hypothesis, which forced us to entertain a different possibility. We hypothesized that mixing altered odor identities such that they were no longer recognizable. Volatile odors generally activate multiple receptors in the olfactory epithelium [15-18]. Odor identity is encoded by the combinatorial activation of glomeruli, mitral/tufted cells in the olfactory bulb and by distributed sets of neurons in the cortices [18-25]. Lateral excitation and inhibition mediated by interconnected neuronal networks may transform receptor activation into more complex population activities.

bioRxiv preprint first posted online Jan. 29, 2020; doi: http://dx.doi.org/10.1101/2020.01.28.923748. The copyright holder for this preprint (which was not peer-reviewed) is the author/funder, who has granted bioRxiv a license to display the preprint in perpetuity. It is made available under a CC-BY-NC-ND 4.0 International license.

We thus conducted a series of experiments to examine neural activities in the olfactory pathway. We first examined the activation of olfactory glomeruli by individual odors and their binary mixtures using the *OMP-IRES-tTA:tetO-GCaMP2* mice [18,26]. Aversive odors including PEA, 2-MBA, IAMM, as well as neutral odors, including HXO and EUG, all activated the dorsal bulb. We presented EUG, 2-MBA and their mixture and recorded glomerular activation (Fig. 2a, b). Mixtures elicited glomerular response patterns similar to the sum of the component odors. We plotted the response amplitude of the mixture against the arithmetic sum of the two individual odors. A simple linear relationship would indicate conformity between the two. The response amplitudes for individual glomeruli were mostly aligned with the diagonal line, indicating that the mixture did not cause overt masking at the level of the OSN (Fig. 2c). The same was observed for another pair of aversive/neutral odors, PEA and HXO (Supplementary Fig. 1a-c), as well as pairs of innately aversive odors including PEA/IAMM (Fig. 2e-g) and PEA/2-MBA (Supplementary Fig. 1e-g). There was no apparent masking of odors in the periphery at the receptor response level that could explain the loss of aversion. We performed linear decoding of the activation patterns. For all the odor pairs we tested, the linear decoding from individual odors can predict the mixture response precisely (Fig. 2d, h and Supplementary Fig. 1d, h).

These observations indicated that odor mixtures could be represented by linear combination of the glomerular responses to individual odors, and that the glomerular representation of the odors were mostly independent of each other. The results were consistent with previous studies of binary odor mixtures [27]. If the insulated labeled line

bioRxiv preprint first posted online Jan. 29, 2020; doi: http://dx.doi.org/10.1101/2020.01.28.923748. The copyright holder for this preprint (which was not peer-reviewed) is the author/funder, who has granted bioRxiv a license to display the preprint in perpetuity. It is made available under a CC-BY-NC-ND 4.0 International license.

hypothesis is correct, this type of superposition would allow each odor to activate its distinctive pathway and elicit aversion.

Altered odor representation by the mitral/tufted cells

To test whether this type of linear separation is carried through the olfactory pathways, we next examined neural activities of the mitral/tufted cells in the olfactory bulb. We performed two-photon calcium imaging experiments in *Cdhr1-Cre* mice injected with an adeno-associated virus (AAV) that expresses the calcium indicator GCaMP6f depending on Cre-mediated recombination (pAAV.Syn.Flex.GCaMP6f.WPRE.SV40) (Fig. 3a) [28]. These mice expressed GCaMP6f specifically in the mitral/tufted cell population (Fig. 3b).

We performed 2-photon imaging to record mitral/tufted cell responses under awake conditions. Odors were presented using the olfactometer to deliver precisely timed stimuli [13]. We recorded 4320 odor/neuron pairs (288 cells and 15 odors) in response to PEA, IAMM, 2-MBA, EUG, HXO and their binary mixtures. The cells exhibited characteristic responses timed to odor stimulations with both increase and decrease in calcium signals (Fig 3c, h and Supplementary Fig. 2a, f).

Quantitative measurements of the responses indicated that cells responding to only one of the two odors responded to the mixture with larger or diminished amplitudes, and these bidirectional changes were observed for both aversive/neutral and aversive/aversive odor pairs (Fig. 3d, e, i, j and Supplementary Fig. 2b, c, g, h). For all odor pairs examined, response amplitude of individual cells to the mixture was smaller overall than the sum of

bioRxiv preprint first posted online Jan. 29, 2020; doi: http://dx.doi.org/10.1101/2020.01.28.923748. The copyright holder for this preprint (which was not peer-reviewed) is the author/funder, who has granted bioRxiv a license to display the preprint in perpetuity. It is made available under a CC-BY-NC-ND 4.0 International license.

responses to the components. This could be seen in pairwise plot of the response amplitudes for aversive/neutral (Fig. 3d, e and Supplementary Fig. 2b, c) and aversive/aversive pairs alike (Fig. 3i, j and Supplementary Fig. 2g, h). It could also be seen as the distribution of amplitude for individual odors and their mixtures. The distribution for the mixtures were similar to those of single odors (Fig. 3f, k and Supplementary Fig. 2d, i). This lack of summation as found in the glomerular response indicated that the overall response was normalized within the cell population.

The patterns of activity that represent the odor mixture were strikingly different from that for individual odors or their sum (Fig. 3e, j and Supplementary Fig. 2c, h). Using linear decoding from individual odor responses, we found that the mixture responses were poorly correlated with the predicted ones, indicating the mixture responses could not be linearly demixed into individual odor patterns (Fig. 3g, l, m and Supplementary Fig. 2e, j). Thus, the population response to the mixture likely represented a new odor identity rather than the combination of two components.

Differential brain activation by aversive odor in mixture

Recordings from the olfactory bulb indicated that the representation of odor identities were likely altered in the mixtures. To evaluate the impact of these changes on other brain areas, we examined the regions shown to be responsible for innate odor-triggered behaviors. The olfactory bulb projects to at least five cortical areas, including the PLCo and the posterior nuclei of the medial amygdala (MeP), where the pathway appeared to diverge and activated different brain regions associated with different valence [29-32] (Fig.

bioRxiv preprint first posted online Jan. 29, 2020; doi: http://dx.doi.org/10.1101/2020.01.28.923748. The copyright holder for this preprint (which was not peer-reviewed) is the author/funder, who has granted bioRxiv a license to display the preprint in perpetuity. It is made available under a CC-BY-NC-ND 4.0 International license.

4a). The bed nucleus of stria terminalis (BST), including the anteriomedial nucleus (BSTMA), mediates anxiogenic response [33,34]. The anterior hypothalamic area, anterior part (AHA) is required to trigger fear responses [33-36]. The ventral MeP (MePV) projects to the ventral medial hypothalamic nucleus (VMH), which has been implicated in both attraction of mouse urine [37,38] and aggressive responses [37].

To quantify the activation of these brain areas, we performed immunofluorescence staining against phospho-S6 ribosomal protein (pS6), which stained activated neurons [39]. Following odor exposure, we performed serial sections through the brain to examine the patterns of activation in different regions. PEA, but not the mixture with HXO, induced strong signals in BST, AHA, VMH, PVA, PLCo and MePV (Fig. 4b, c). This observation suggested that areas associated with odor valence were differentially activated by an innately aversive odor depending on whether it was presented alone or in a mixture. The lack of activation by the mixtures was consistent with the lack of induced aversion. On the other hand, the number of cells activated in the basolateral amygdala (BLA) and the piriform cortex (Pir) were not significantly different (Fig. 4b, c). Thus, areas that receive olfactory input, though not known to be particularly associated with valence, were similarly activated.

We then compared the brain activation patterns elicited by the mixture of two aversive odors with that activated by the aversive odors alone. Even though both PEA and IAMM activated the BST, VMH and PLCo, the PEA/IAMM mixture did not (Fig. 4b, d). The lack of activation of these areas was consistent with the behavioral test results.

bioRxiv preprint first posted online Jan. 29, 2020; doi: http://dx.doi.org/10.1101/2020.01.28.923748. The copyright holder for this preprint (which was not peer-reviewed) is the author/funder, who has granted bioRxiv a license to display the preprint in perpetuity. It is made available under a CC-BY-NC-ND 4.0 International license.

Distinguishing aversive odors from background

It is counterintuitive that mixing an aversive odor with a neutral odor abolished aversive response. Animals react to predator or food odors in complex odiferous environments, suggesting that they can identify these odors in presence of background odors. In our experiments involving odor mixtures, the two odors were presented contemporaneously. In natural environment, individual odors arrive at the nostril as plumes. The aversive odors could be detected with spatial-temporal displacement from environmental smells and be perceived as distinct. Thus, experimentally introducing temporal or spatial displacement in the presentation of the background odor may allow the aversive odors to be detected as their own in the mixture. We tested this hypothesis presenting a neutral odor as background, followed by the mixture, and tested the innate response to the mixture (Fig. 5a). In experiments using PEA with HXO, and using 2-MBA with eugenol, we found that the mixtures elicited the same level of aversion as the aversive odors alone (Fig. 5b, c). Thus, background presentation of the neutral odors allowed PEA or 2-MBA within the mixtures to be properly recognized. Temporally displaced presentation of odors was sufficient to allow individual odors to be distinguished whereas well-mixed odors are not.

We next recorded glomerular responses to the mixture after presenting the neutral odor as background. We first recorded the responses to individual component odors and to the mixtures. The recording provided points for comparison. We then presented the neural odor as background, followed by the mixture, and recorded the response to the mixture.

bioRxiv preprint first posted online Jan. 29, 2020; doi: http://dx.doi.org/10.1101/2020.01.28.923748. The copyright holder for this preprint (which was not peer-reviewed) is the author/funder, who has granted bioRxiv a license to display the preprint in perpetuity. It is made available under a CC-BY-NC-ND 4.0 International license.

Following background presentation, the mixtures elicited responses that were dissimilar to those by mixtures alone. The overall patterns were similar to the innately aversive odors alone (Fig. 5d-g). For individual glomeruli, the responses exhibited similar temporal dynamics and amplitude to that elicited by the aversive odors alone (Fig. 5d-g). Linear decoding indicated that the mixtures elicited a response that can be predicted as the aversive odors (Fig. 5h-i).

We also performed imaging of the mitral/tufted cells to monitor the response to the mixture after the neutral odor was presented as a background. Without background odor presentation, the mitral cell activity elicited by the mixture was poorly correlated with the pattern elicited by the aversive odor alone (Fig. 5j, k). However, when the neutral odor was presented as background, the mixture elicited responses that were highly correlated with the aversive odors (Fig. 5l, m). For individual cells, the dynamics and amplitude of the responses elicited by the mixture were similar to those elicited by the aversive odors (Fig. 5n, o). Linear decoding indicating that mixtures presented over background were more likely linearly decoded as the aversive odors than the mixture alone (Fig. 5p, q). These adapted responses offered an explanation of the behavioral response to the mixture when presented over background.

Discussion

Innate responses to some environmental stimuli are shaped by evolution to afford animals survival advantages even without learning. Because of the inborn nature of these

bioRxiv preprint first posted online Jan. 29, 2020; doi: http://dx.doi.org/10.1101/2020.01.28.923748. The copyright holder for this preprint (which was not peer-reviewed) is the author/funder, who has granted bioRxiv a license to display the preprint in perpetuity. It is made available under a CC-BY-NC-ND 4.0 International license.

responses, information about innately recognized cues is thought to be processed using circuits different from those for stimuli that can be learned by their association with unconditioned reward or punishment. Labeled lines, such as those mediating looming-induced flight response and spinal cord reflexes, provide a simple solution by linking sensory cells and behavioral centers (Fig. 6a). Our results show that mixtures abolish innate aversive response. The most striking is that observation that mixing two odors with the same valence also abolishes innate responses. These observations cannot be simply explained by opposing actions of brain centers that drive different behaviors. Nor can it be accounted for by peripheral masking or antagonist interactions of ligands with the receptors [40]. Past studies have shown that presynaptic responses elicited by odor mixture were mostly mediated by intraglomerular interactions [27,41,42]. Consistent with these studies, glomerular responses to the mixtures can be linearly separated into those elicited by the component odors.

In contrast, mixtures elicit responses in the mitral/tufted cell population that no longer conform to the individual channels that convey information of the component odors independently. This result differs from a previous study indicating that component mixtures can be linearly decoded using the mitral cell responses [43]. The result does not fit the classic labeled line model where straightforward relays of information through the lines elicit stereotypical behaviors. Rather, they suggest that the highly interconnected networks in the mammalian olfactory pathway have a strong influence on how the innately recognized odors are encoded.

bioRxiv preprint first posted online Jan. 29, 2020; doi: http://dx.doi.org/10.1101/2020.01.28.923748. The copyright holder for this preprint (which was not peer-reviewed) is the author/funder, who has granted bioRxiv a license to display the preprint in perpetuity. It is made available under a CC-BY-NC-ND 4.0 International license.

Odor identities are encoded by the ensemble activity of neurons in the olfactory pathway. Natural odors are usually blend of individual odorant chemicals. Since individual chemicals activate multiple glomeruli and corresponding mitral cells, additive response from multiple chemicals in a blend would quickly saturate the responses. This problem is solved by presynaptic inhibition that is mostly intraglomerular, as well as by inhibition among the mitral/tufted cells. Notably, interactions among the mitral/tufted cell population are mediated by inhibitory interneurons that are no long restricted to intraglomerular interactions [44]. The interglomerular interactions not only can normalize mitral cells response, they also can redistribute the patterns. In many cases, an odor blend creates a configural (synthetic) rather than elemental (analytical) perception [45,46]. The redistribution of mitral/tufted responses likely underlie the configural perception because the patterns elicited by the mixtures are treated as new rather than the combination of two separate known odors.

However, such redistribution has not been demonstrated for innately recognized odors in a blend. Our recorded mitral/tufted cell responses clearly show non-linear interactions, which not only resulted in redistributed amplitude that appeared to have been normalized, but also resulted in patterns of activities that are likely perceived as novel to the animals. The results, therefore, suggest that the activity triggered by innately recognized odors are not insulated from those of others. In contrast, they are encoded similarly as all other odors, through a generalized population code resulting from interactions among the mitral/tufted cells.

bioRxiv preprint first posted online Jan. 29, 2020; doi: http://dx.doi.org/10.1101/2020.01.28.923748. The copyright holder for this preprint (which was not peer-reviewed) is the author/funder, who has granted bioRxiv a license to display the preprint in perpetuity. It is made available under a CC-BY-NC-ND 4.0 International license.

If these innately recognized odors are encoded by a general population code, how are their valence assigned? Although the classic labeled line model (Fig. 6a) provides a simple way of understanding intrinsic values associated, it is difficult to envision how it may operate with population activities that are subject to influence by other odors. Odor valence can be assigned through associative learning, presumably by associating patterns of activity that encode the odors with an unconditioned stimulus (reward or punishment) to assign valence (Fig. 6b). We reason that innate odor may be similar in the sense that the neurons that carry population activity associated with innately recognized odors are connected to neurons that preferentially drive attraction or aversion (Fig. 6c). The difference is that this association is intrinsically determined rather than acquired through associative learning. This model allows genetic programs to specify the neurons that encode odor identities, as well as their connection with valence circuit. In contrast to the labeled lines, this model does not require neurons that encode innately recognized odors to be specifically tuned, nor does it require the activity encoding odor identities to be insulated from the influence of other odors. When the pattern of activity associated with an innately recognized odor is altered by mixing with another odor, the ensemble activity creates a novel odor identity and abolishes the valence associated with the component odor (Fig. 6d). Activity-dependent modification of how olfactory sensory neurons project to the olfactory bulb during development would also alter these predisposed connections and change the valence associated with the odors (Fig. 6e) [12].

This model can also explain the recognition of odors in the presence of background odors. When the odor presentation is temporally or spatially displaced from the

bioRxiv preprint first posted online Jan. 29, 2020; doi: http://dx.doi.org/10.1101/2020.01.28.923748. The copyright holder for this preprint (which was not peer-reviewed) is the author/funder, who has granted bioRxiv a license to display the preprint in perpetuity. It is made available under a CC-BY-NC-ND 4.0 International license.

background, individual odors in the mixture can be distinguished as distinct and their associated valence remain intact [47]. In this sense, innate detection of ethologically relevant odors is a form of elemental perception that requires their presentation to be independent from the environment. This model, therefore, allows a general coding strategy for all odors alike and permit flexible assignment of valence to neutral odors or reassign valence to those with intrinsic preference.

bioRxiv preprint first posted online Jan. 29, 2020; doi: http://dx.doi.org/10.1101/2020.01.28.923748. The copyright holder for this preprint (which was not peer-reviewed) is the author/funder, who has granted bioRxiv a license to display the preprint in perpetuity. It is made available under a CC-BY-NC-ND 4.0 International license.

Methods

Animals

The *OMP-IRES-tTA* (Jackson laboratory, JAX: 017754), *tetO-GCaMP2* (Jackson laboratory, JAX: 017755), and *Cdhr1-Cre* (MMRRC, 030952-UCD) mice were described previously [18,26,48]. The C57BL/6J (Jackson laboratory, JAX: 000664) were used for control group. All the animals were maintained in Lab Animal Services Facility of Stowers Institute at 12:12 hour reversed light cycle and provided with food and water *ad libitum*. All the behavior and functional imaging experiments were conducted during the dark light cycle under red or infrared light illumination. Experimental protocols involving mice were approved by the Institutional Animal Care and Use Committee at Stowers Institute and in compliance with the NIH Guide for Care and Use of Animals.

Odor delivery with olfactometer

Odor delivery was controlled by an automated olfactometer with custom written software developed in the National Instrument Labview programming environment [13]. Odorant chemicals are including: 2-Hexanone (Abbr: HXO), Heptanal (Abbr: HPH), Eugenol (Abbr: EUG), 2-Methylbutyric acid (Abbr: 2-MBA), 2-phenylethylamine (Abbr: PEA) , isoamylamine (Abbr: IAMM) and were purchased from MilliporeSigma and freshly prepared in mineral oil at desired concentration. Female mouse urine (fresh collected from C57BL/6J mice, Abbr: FU), Male mouse urine (fresh collected from C57BL/6J mice, Abbr: MU), Coyote urine (Abbr: CU), Peanut butter (Jif Extra Crunchy, Abbr: PB), Maple flavor (Frontier natural products co-op, Abbr: Maple), Lemon flavor (Frontier natural products co-op, Abbr: lemon) were used at original concentration. Odorants were then further diluted in carrier air with a maintained total flow rate (400 ml/min for calcium imaging and 100ml/min for behavior experiments).

Innate odor preference test

bioRxiv preprint first posted online Jan. 29, 2020; doi: http://dx.doi.org/10.1101/2020.01.28.923748. The copyright holder for this preprint (which was not peer-reviewed) is the author/funder, who has granted bioRxiv a license to display the preprint in perpetuity. It is made available under a CC-BY-NC-ND 4.0 International license.

Experiments are the same as previously described [13]. 2-4-month-old mice were used for cross habituation experiments. Each experimental group contained 10-14 animals. Unless otherwise stated, all animals were naïve to the testing odors and exposed to the same odor once. Each animal was tested with a total of two separate experiments with at least one week between tests. After being habituated to the testing environment for half an hour, the animals were put into a 20cm x 20cm chamber for behavioral experiments. Odors from the olfactometer were delivered through a nose cone on one of the side walls, which is 5 cm above the base plate. A vacuum tube connected on the opposite wall of the nose cone provided an air flow to remove residual odors after odor delivery. Pure odorants were diluted into mineral oil at $1{:}10^3$ (v/v) in most cases. 10 ml/min air flow carried the saturated odor out from the odor vial and was further diluted into a 90 ml/min carrier air to make the final dilution to 10^{-4} (v/v). Delivery time, concentration and sequence of odor delivery were controlled by the olfactometer software. Investigation of odor source was registered by infrared beam breaking events and recorded by the same software that controlled the olfactometer.

The sequence of trial sessions is depicted in Fig. 1. Odor was delivered for 5 minutes in each trial. After four trials of mineral oil presentation, a testing odor was presented 4 times. In a typical test, mice habituating to the test chambers over the multiple sessions of background air led to decreased T_{Air}. The presentation of an odor elicited an increased T_{Odor}. Repeated presentation of the same odor led to habituation, which was reversed by the test odor if it was perceived as novel. If the odor is attractive to the animal, an increased T_{Odor1} is expected as the mixed result of novelty and attraction. If the odor is avoided by the animal, a smaller increase or even decrease T_{Odor1} is expected as the mixed result of novelty seeking (risk assessment) and avoidance, while the T_{Odor2} is expected as the aversion only because the novelty is habituated quickly while the avoidance persists longer. We define the following indices:

$$\text{attraction index} = \frac{T_{Odor1} - T_{Air4}}{T_{Ave.Air}} \times 100$$

bioRxiv preprint first posted online Jan. 29, 2020; doi: http://dx.doi.org/10.1101/2020.01.28.923748. The copyright holder for this preprint (which was not peer-reviewed) is the author/funder, who has granted bioRxiv a license to display the preprint in perpetuity. It is made available under a CC-BY-NC-ND 4.0 International license.

$$\text{aversion index} = \frac{T_{Air4} - T_{Odor2}}{T_{Ave.Air}} \times 100$$

Odors used in innate behavior experiments were as follows: FU, MU, CU, PB, maple, lemon. These odors were delivered without dilution. PEA, IAMM, 2-MBA, HPH, HXO and EUG were diluted at 1:1000 in mineral oil. All the odors were then further diluted in the olfactometer in the air phase for another 10-fold.

Phospho-S6 mapping of odor-evoked activity

For mixture phospho-S6 staining, animals were single housed and habituated in home cages for seven days with a glass vial covered with a plastic cover, which was punched with seven holes for odor evaporation while preventing physical contact with chemicals. For habituation, a small piece of cotton nestlet soaked with 500 µl mineral oil was put inside the vial. Vials were changed every day at one hour after light cycle. In day eight, a new glass vial with cotton nestlet soaked with 500 µl 2-MBA, PEA, IAMM, HXO or EUG at $1{:}10^3$ dilution in mineral oil, or freshly collected male or female urine was added in the home cages. Binary mixtures were prepared with equal mix of two odors. One hour after odor stimulation, mice were sacrificed and perfused with 4% PFA. The mouse brains were dissected and post-fixed with 4% PFA overnight at 4ºC.

The phospho-S6 immunochemistry histology was performed based on the published protocol [39] with some modifications. The entire brain was cut into 50 µm thick serial sections using a Leica vibratome (VT1000S). Rabbit anti phospho-S6 antibody (Cell Signaling, Cat#: 4854) was diluted 1:1000 in 0.1% PBST (0.1% Triton X-100 in 1X PBS) and used to incubate the slices at 4 ºC overnight. The 3-p peptide (25 nM biotin-QIAKRRRLpSpSLRApSTSKSESSQK, where pS is phosphoserine; synthesized by United Peptide) was also included to reduce background staining [39]. Donkey anti-Rabbit 488 was (Thermo Fisher Scientific, Cat#: R37118;) diluted to 1:1000 in PBST for

bioRxiv preprint first posted online Jan. 29, 2020; doi: http://dx.doi.org/10.1101/2020.01.28.923748. The copyright holder for this preprint (which was not peer-reviewed) is the author/funder, who has granted bioRxiv a license to display the preprint in perpetuity. It is made available under a CC-BY-NC-ND 4.0 International license.

secondary antibody staining overnight. DAPI (Thermo Fisher Scientific, Cat#: D1306) was used for nuclear staining.

Tiled images were acquired using Olympus VS120 Virtual Slide Microscope or PE Ultraview spinning disk confocal microscope (PerkinElmer), which were stitched together using the Volocity software (PerkinElmer). Different brain nuclei were identified based on the brain atlas (The Mouse Brain Stereotaxic Coordinates, third edition). The pS6 immuno-positive neurons were counted using ImageJ. For quantification, the two sides of the brain were treated independently and the following numbers of sections were used: anterior hypothalamic area, anterior part (AHA), 4 sections at -0.85~-1.05 mm from Bregma; medial amygdaloid nucleus (posterodorsal area, MePD, and posteroventral area, MePV) and ventromedial hypothalamic nucleus (ventrolateral area; VMHvl), 5 sections between -1.35~-1.60 mm from Bregma; hypothalamic nucleus (VMH) in the 2-MBA case, 4 sections between -1.80~-2.00 mm from Bregma; bed nucleus of the stria terminalis (BST), 3 sections between 0.10~0.25 mm from Bregma; posterolateral cortical amygdaloid area (PLCo), 5 sections at -1.35~-1.60 mm from Bregma; paraventricular thalamic nucleus (PVA), 4 sections at -0.25~-0.45 mm from Bregma ; piriform cortex (Pri), 5 sections at -1.35~-1.60 mm from Bregma; basolateral amygdaloid nucleus, anterior part (BLA), 5 sections at -1.10~-1.35 mm from Bregma.

Awake head fixed calcium imaging

For calcium imaging of glomerulus, generation of the GCaMP2 mice was described previously [26]. Line 12i and 5i mice that exhibited strong fluorescence were used for imaging experiments as described previously [18]. One day prior to imaging, mice were anesthetized by intraperitoneal injection of ketamine/xylazine cocktail (100mg/kg, 10mg/kg body weight respectively) for surgery with thinned skull above the olfactory bulb.

bioRxiv preprint first posted online Jan. 29, 2020; doi: http://dx.doi.org/10.1101/2020.01.28.923748. The copyright holder for this preprint (which was not peer-reviewed) is the author/funder, who has granted bioRxiv a license to display the preprint in perpetuity. It is made available under a CC-BY-NC-ND 4.0 International license.

For 2-photon mitral/tufted cell imaging, *Cdhr1-Cre* mice were anesthetized, and two small holes were made above each side of anterior and posterior olfactory bulb for virus injection. At each injection site, 250 nl pAAV.Syn.Flex.GCaMP6f.WPRE.SV40 virus (Addgene, 100833-AAV1) was injected into mitral cell layer at both 200 µm and 300 µm depths (Chen et al., 2013). After 3-4 weeks, animals were anesthetized to open a craniotomy window over the olfactory bulb and a 3 mm diameter glass cover slip was attached to the skull using dental cement. Animals were used for calcium imaging the next day.

Odorants were diluted in mineral oil ($1:10^2$) and delivered at 40 ml/min flow rate. Total flow rate was maintained at 400 ml/min in all experiments. For the mixtures, both odors were delivered at 40ml/min and mixed inside the olfactometer before delivered to the mouse nose. Odors were delivered for 3 seconds followed by a 27 second interval.

For GCaMP2 glomeruli imaging, responses to odor stimuli were collected on an Olympus BX60WI microscope using 4X air lens (Olympus XLFLUOR4X/340, NA 0.28). The image was collected at 512x512 resolution with 2x2 bin with sampling rate at 8.3 Hz. For mitral cell 2-photon imaging, the image was collected by an Olympus 2-photon microscope (FLUOVIEW FVMPE-RS) with 940 nm emission laser using 25X water lens (Olympus XLPLN25XWMP, NA 1.05). A resonate scanner with GaAsP detector was used for image collection at 512x512 resolution with 15 Hz sampling rate. Animals were head-fixed and freely standing on a roller during the experiment.

Custom-written scripts in ImageJ and MATLAB (Mathworks) were used for image processing as described previously [18]. Briefly, after ROIs were manually defined, the averaged response inside each ROI was extracted by ImageJ. Using customized MATLAB software, a baseline was defined for each ROI and $\Delta F/F$ was calculated. To display the response patterns, the peak amplitude of each glomerulus was mapped onto the spatial location of the glomerulus. The value was presented by applying a Gaussian blur with 50 µm standard deviation.

bioRxiv preprint first posted online Jan. 29, 2020; doi: http://dx.doi.org/10.1101/2020.01.28.923748. The copyright holder for this preprint (which was not peer-reviewed) is the author/funder, who has granted bioRxiv a license to display the preprint in perpetuity. It is made available under a CC-BY-NC-ND 4.0 International license.

Quantification and statistical analysis

All the statistics are conducted in MATLAB or OriginPro. Data were expressed as means ± SEMs in figures and text. Group differences were analyzed using one-way Student *t*-test. Significance was defined as: * indicates $p < 0.05$, ** indicates $p < 0.01$, *** indicates $p < 0.001$. ns indicates $p > 0.05$. MATLAB build in function 'linsolve' was used for the linear decoding analysis. It solves the linear system A*X = B using LU factorization with partial pivoting when A is square and QR factorization with column pivoting otherwise. A is the glomeruli's or mitral cells' responses to the two component odorants; B is the response to the mixture. A*X then was used to plot against B for a correlation analysis. A lower correlation coefficient indicates poor linear decoding.

Acknowledgments

We thank A. Moran and members of the Lab Animal Services at the Stowers Institute for technical assistance. We also thank valuable input from members of the Yu laboratory. The work is supported by funding from Stowers Institute and the NIH (R01DC 008003, R01DC 014701 and R01DC016696).

Ethics declarations

Competing interests

The authors declare no competing interests.

bioRxiv preprint first posted online Jan. 29, 2020; doi: http://dx.doi.org/10.1101/2020.01.28.923748. The copyright holder for this preprint (which was not peer-reviewed) is the author/funder, who has granted bioRxiv a license to display the preprint in perpetuity. It is made available under a CC-BY-NC-ND 4.0 International license.

References

1 Kobayakawa, K. *et al.* Innate versus learned odour processing in the mouse olfactory bulb. *Nature* **450**, 503-508 (2007).

2 Fendt, M., Endres, T., Lowry, C. A., Apfelbach, R. & McGregor, I. S. TMT-induced autonomic and behavioral changes and the neural basis of its processing. *Neuroscience & Biobehavioral Reviews* **29**, 1145-1156 (2005).

3 Dewan, A., Pacifico, R., Zhan, R., Rinberg, D. & Bozza, T. Non-redundant coding of aversive odours in the main olfactory pathway. *Nature* **497**, 486-489 (2013).

4 Liberles, S. D. & Buck, L. B. A second class of chemosensory receptors in the olfactory epithelium. *Nature* **442**, 645-650 (2006).

5 Ferrero, D. M. *et al.* Detection and avoidance of a carnivore odor by prey. *Proceedings of the National Academy of Sciences* **108**, 11235 (2011).

6 Li, Q. & Liberles, Stephen D. Aversion and Attraction through Olfaction. *Current Biology* **25**, R120-R129 (2015).

7 Pérez-Gómez, A. *et al.* Innate Predator Odor Aversion Driven by Parallel Olfactory Subsystems that Converge in the Ventromedial Hypothalamus. *Current Biology* **25**, 1340-1346 (2015).

8 Zhang, J., Pacifico, R., Cawley, D., Feinstein, P. & Bozza, T. Ultrasensitive detection of amines by a trace amine-associated receptor. *J Neurosci* **33**, 3228-3239 (2013).

9 Lin, D. Y., Zhang, S. Z., Block, E. & Katz, L. C. Encoding social signals in the mouse main olfactory bulb. *Nature* **434**, 470-477 (2005).

10 Igarashi, K. M. *et al.* Parallel mitral and tufted cell pathways route distinct odor information to different targets in the olfactory cortex. *J Neurosci* **32**, 7970-7985 (2012).

11 Iurilli, G. & Datta, S. R. Population Coding in an Innately Relevant Olfactory Area. *Neuron* **93**, 1180-1197.e1187 (2017).

12 Qiu, Q., Wu, Y., Ma, L. & Yu, C. R. Acquisition of Innate Odor Preference Depends on Spontaneous and Experiential Activities During Critical Period. *bioRxiv*, 2020.2001.2028.923722 (2020).

13 Qiu, Q. *et al.* Automated analyses of innate olfactory behaviors in rodents. *PLoS One* **9**, e93468 (2014).

14 Han, W. *et al.* A Neural Circuit for Gut-Induced Reward. *Cell* **175**, 665-678.e623 (2018).

15 Nara, K., Saraiva, L. R., Ye, X. & Buck, L. B. A large-scale analysis of odor coding in the olfactory epithelium. *J Neurosci* **31**, 9179-9191 (2011).

16 Malnic, B., Hirono, J., Sato, T. & Buck, L. B. Combinatorial receptor codes for odors. *Cell* **96**, 713-723 (1999).

17 Araneda, R. C., Kini, A. D. & Firestein, S. The molecular receptive range of an odorant receptor. *Nat Neurosci* **3**, 1248-1255 (2000).

bioRxiv preprint first posted online Jan. 29, 2020; doi: http://dx.doi.org/10.1101/2020.01.28.923748. The copyright holder for this preprint (which was not peer-reviewed) is the author/funder, who has granted bioRxiv a license to display the preprint in perpetuity. It is made available under a CC-BY-NC-ND 4.0 International license.

18 Ma, L. *et al.* Distributed representation of chemical features and tunotopic organization of glomeruli in the mouse olfactory bulb. *Proc Natl Acad Sci U S A* **109**, 5481-5486 (2012).

19 Bozza, T., McGann, J. P., Mombaerts, P. & Wachowiak, M. In vivo imaging of neuronal activity by targeted expression of a genetically encoded probe in the mouse. *Neuron* **42**, 9-21 (2004).

20 Uchida, N., Takahashi, Y. K., Tanifuji, M. & Mori, K. Odor maps in the mammalian olfactory bulb: domain organization and odorant structural features. *Nat Neurosci* **3**, 1035-1043 (2000).

21 Leon, M. & Johnson, B. Functional units in the olfactory system. *Proc Natl Acad Sci U S A* **103**, 14985-14986 (2006).

22 Soucy, E. R., Albeanu, D. F., Fantana, A. L., Murthy, V. N. & Meister, M. Precision and diversity in an odor map on the olfactory bulb. *Nat Neurosci* **12**, 210-220 (2009).

23 Stettler, D. D. & Axel, R. Representations of odor in the piriform cortex. *Neuron* **63**, 854-864 (2009).

24 Miura, K., Mainen, Z. F. & Uchida, N. Odor representations in olfactory cortex: distributed rate coding and decorrelated population activity. *Neuron* **74**, 1087-1098 (2012).

25 Poo, C. & Isaacson, J. S. Odor representations in olfactory cortex: "sparse" coding, global inhibition, and oscillations. *Neuron* **62**, 850-861 (2009).

26 He, J., Ma, L., Kim, S., Nakai, J. & Yu, C. R. Encoding gender and individual information in the mouse vomeronasal organ. *Science* **320**, 535-538 (2008).

27 McGann, J. P. *et al.* Odorant representations are modulated by intra- but not interglomerular presynaptic inhibition of olfactory sensory neurons. *Neuron* **48**, 1039-1053 (2005).

28 Chen, T.-W. *et al.* Ultrasensitive fluorescent proteins for imaging neuronal activity. *Nature* **499**, 295 (2013).

29 Brennan, P. A. & Kendrick, K. M. Mammalian social odours: attraction and individual recognition. *Philos Trans R Soc Lond B Biol Sci* **361**, 2061-2078 (2006).

30 Yoon, H., Enquist, L. W. & Dulac, C. Olfactory inputs to hypothalamic neurons controlling reproduction and fertility. *Cell* **123**, 669-682 (2005).

31 Kang, N., Baum, M. J. & Cherry, J. A. A direct main olfactory bulb projection to the 'vomeronasal' amygdala in female mice selectively responds to volatile pheromones from males. *Eur J Neurosci* **29**, 624-634 (2009).

32 Boehm, U., Zou, Z. & Buck, L. B. Feedback loops link odor and pheromone signaling with reproduction. *Cell* **123**, 683-695 (2005).

33 Duvarci, S., Bauer, E. P. & Pare, D. The bed nucleus of the stria terminalis mediates inter-individual variations in anxiety and fear. *J Neurosci* **29**, 10357-10361 (2009).

34 Kim, S. Y. *et al.* Diverging neural pathways assemble a behavioural state from separable features in anxiety. *Nature* **496**, 219-223 (2013).

bioRxiv preprint first posted online Jan. 29, 2020; doi: http://dx.doi.org/10.1101/2020.01.28.923748. The copyright holder for this preprint (which was not peer-reviewed) is the author/funder, who has granted bioRxiv a license to display the preprint in perpetuity. It is made available under a CC-BY-NC-ND 4.0 International license.

35 Gross, C. T. & Canteras, N. S. The many paths to fear. *Nat Rev Neurosci* **13**, 651-658 (2012).

36 Canteras, N. S., Ribeiro-Barbosa, E. R. & Comoli, E. Tracing from the dorsal premammillary nucleus prosencephalic systems involved in the organization of innate fear responses. *Neurosci Biobehav Rev* **25**, 661-668 (2001).

37 Lin, D. *et al.* Functional identification of an aggression locus in the mouse hypothalamus. *Nature* **470**, 221-226 (2011).

38 Yang, C. F. *et al.* Sexually dimorphic neurons in the ventromedial hypothalamus govern mating in both sexes and aggression in males. *Cell* **153**, 896-909 (2013).

39 Knight, Z. A. *et al.* Molecular profiling of activated neurons by phosphorylated ribosome capture. *Cell* **151**, 1126-1137 (2012).

40 Saraiva, L. R. *et al.* Combinatorial effects of odorants on mouse behavior. *Proceedings of the National Academy of Sciences* **113**, E3300-E3306 (2016).

41 Murphy, G. J., Darcy, D. P. & Isaacson, J. S. Intraglomerular inhibition: signaling mechanisms of an olfactory microcircuit. *Nat Neurosci* **8**, 354-364 (2005).

42 Dhawale, A. K., Hagiwara, A., Bhalla, U. S., Murthy, V. N. & Albeanu, D. F. Non-redundant odor coding by sister mitral cells revealed by light addressable glomeruli in the mouse. *Nat Neurosci* **13**, 1404-1412 (2010).

43 Fletcher, M. L. Analytical processing of binary mixture information by olfactory bulb glomeruli. *PLoS One* **6**, e29360 (2011).

44 Economo, Michael N., Hansen, Kyle R. & Wachowiak, M. Control of Mitral/Tufted Cell Output by Selective Inhibition among Olfactory Bulb Glomeruli. *Neuron* **91**, 397-411 (2016).

45 Gottfried, J. A. Central mechanisms of odour object perception. *Nat Rev Neurosci* **11**, 628-641 (2010).

46 Frederick, D. E., Barlas, L., Ievins, A. & Kay, L. M. A critical test of the overlap hypothesis for odor mixture perception. *Behav Neurosci* **123**, 430-437 (2009).

47 Gschwend, O. *et al.* Neuronal pattern separation in the olfactory bulb improves odor discrimination learning. *Nat Neurosci* **18**, 1474-1482 (2015).

48 Nagai, Y., Sano, H. & Yokoi, M. Transgenic expression of Cre recombinase in mitral/tufted cells of the olfactory bulb. *genesis* **43**, 12-16 (2005).

bioRxiv preprint first posted online Jan. 29, 2020; doi: http://dx.doi.org/10.1101/2020.01.28.923748. The copyright holder for this preprint (which was not peer-reviewed) is the author/funder, who has granted bioRxiv a license to display the preprint in perpetuity. It is made available under a CC-BY-NC-ND 4.0 International license.

Figures

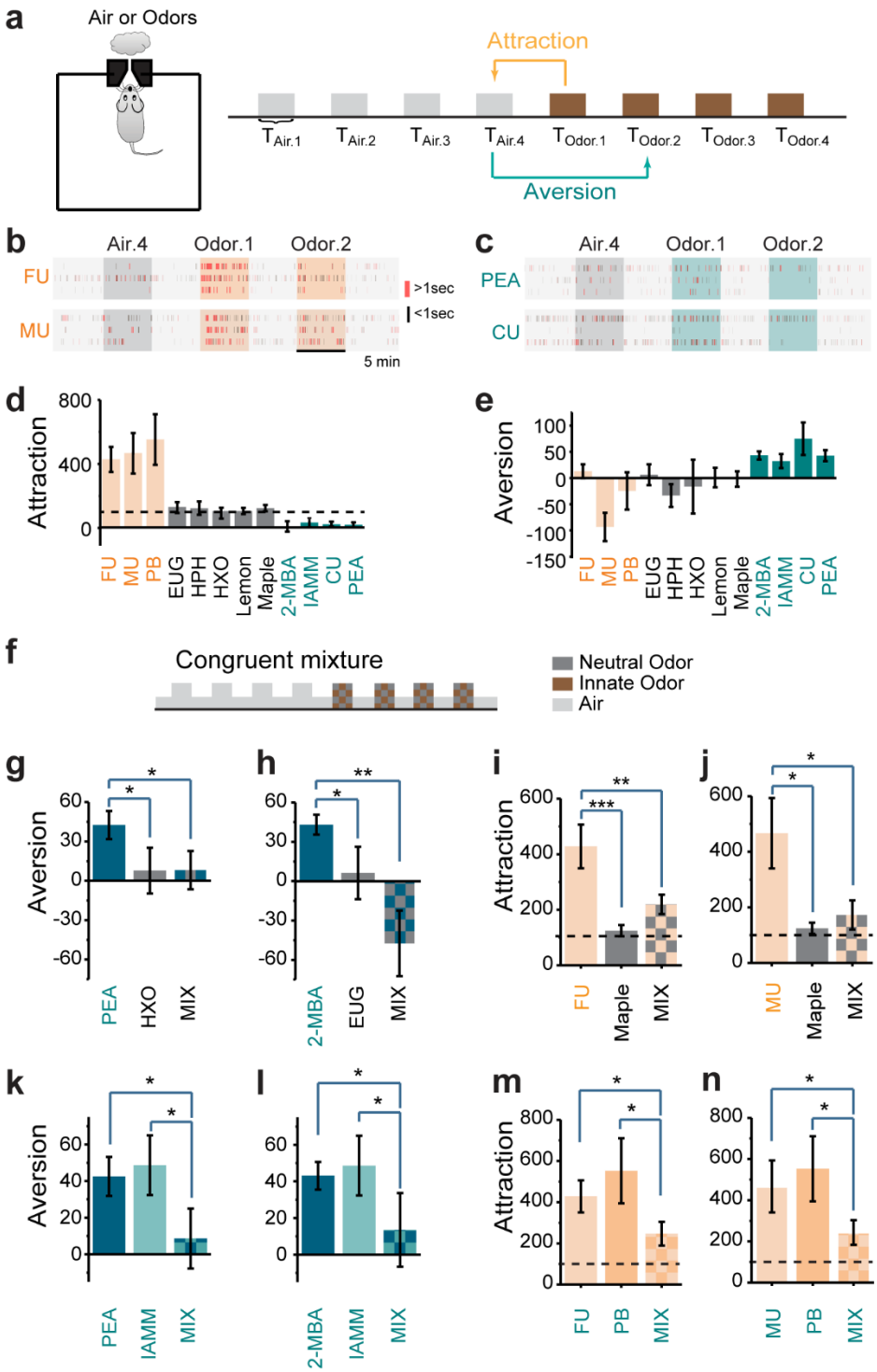

bioRxiv preprint first posted online Jan. 29, 2020; doi: http://dx.doi.org/10.1101/2020.01.28.923748. The copyright holder for this preprint (which was not peer-reviewed) is the author/funder, who has granted bioRxiv a license to display the preprint in perpetuity. It is made available under a CC-BY-NC-ND 4.0 International license.

Fig. 1: Odor mixtures abolish innate odor preference

a Illustration of the behavior paradigm. Left, single odor port arena. Right, odor presentation sequence and the quantification of attraction and aversion.

b Raster plots of odor port investigation (three animals each) of air, female or male urine (FU and MU) presentation. Only the fourth air presentation (Air.4, gray box) and the first two odor presentations (Odor.1 and Odor.2, orange boxes) are shown. Each tick represents an investigation event. Investigations longer or shorter than 1 second are marked by red and black ticks, respectively.

c Same as **b** but for 2-phenylethylamine (PEA) and coyote urine (CU). Olive colored boxes indicating presentation of aversive odors.

d Bar graphs showing attractive response for a panel of odors (attractive: orange; neutral: gray; aversive: olive). Dashed line indicating the level for neutral odors.

e Bar graphs showing aversion response for the same odors in **d**.

f Illustration of congruent mixture experiment setup.

g, h Bar plots of aversion measured for PEA, HXO and their mixture (MIX, **g**), and 2-MBA, EUG and their mixture (**h**).

i, j Bar plots of attraction measured for female urine, maple and the mixture (**i**), and male urine, maple and their mixture (**j**).

k, l Bar plots of average aversion indices to PEA, IAMM and their mixture (**k**), and 2-MBA, IAMM and their mixture (**l**).

m, n Bar plots of average attraction indices to female urine, peanut butter and mixture (**m**), and male urine, peanut butter and their mixture (**n**). Dashed line indicating the level for neutral odors.

Abbreviation: FU: female urine; MU: male urine; PB: peanut butter; EUG: eugenol; HPH: heptanal; HXO: 2-hexanone; IAMM: isoamylamine; CU: cayote urine; 2-MBA: 2-Methylbutyric acid; PEA: 2-phenylethylamine. One-way student *t*-test applied, * indicates $p < 0.05$, ** indicates $p < 0.01$, *** indicates $p < 0.001$. ns indicates $p > 0.05$. All bar graph data are shown in mean ± SEM.

bioRxiv preprint first posted online Jan. 29, 2020; doi: http://dx.doi.org/10.1101/2020.01.28.923748. The copyright holder for this preprint (which was not peer-reviewed) is the author/funder, who has granted bioRxiv a license to display the preprint in perpetuity. It is made available under a CC-BY-NC-ND 4.0 International license.

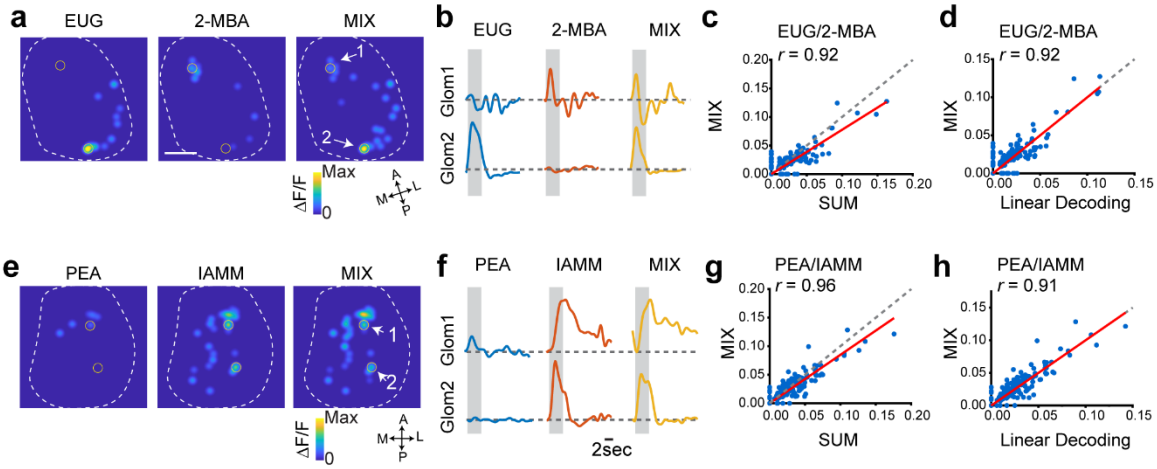

Fig. 2: Linear decoding of odors from glomeruli responses

a Glomerular activation patterns elicited by EUG, 2-MBA and their mixture. Contours of the bulb are outlined. Two of glomeruli are labelled. Orientations of the bulb are labeled as: A: anterior; P: posterior; M: medial; L: lateral. Scale bar, 500 µm.

b Sample traces from the labelled glomeruli from **a**. Grey box indicates the odor presentation.

c Scatter plot of glomerular response amplitude evoked by the mixture against the sum of response amplitudes to individual odors. Red line indicates linear fit of the data. Correlation coefficient (*r*) and diagonal line (grey dot) are indicated.

d Scatter plot of response of individual glomeruli to the mixture against the predicted response from linear decoding for odor pair EUG/2-MBA. Red line indicates linear fit of the data. Correlation coefficient (*r*) and diagonal line (grey dot) are indicated.

e-h Same as **a-d**, but for two aversive odor pair PEA/IAMM.

bioRxiv preprint first posted online Jan. 29, 2020; doi: http://dx.doi.org/10.1101/2020.01.28.923748. The copyright holder for this preprint (which was not peer-reviewed) is the author/funder, who has granted bioRxiv a license to display the preprint in perpetuity. It is made available under a CC-BY-NC-ND 4.0 International license.

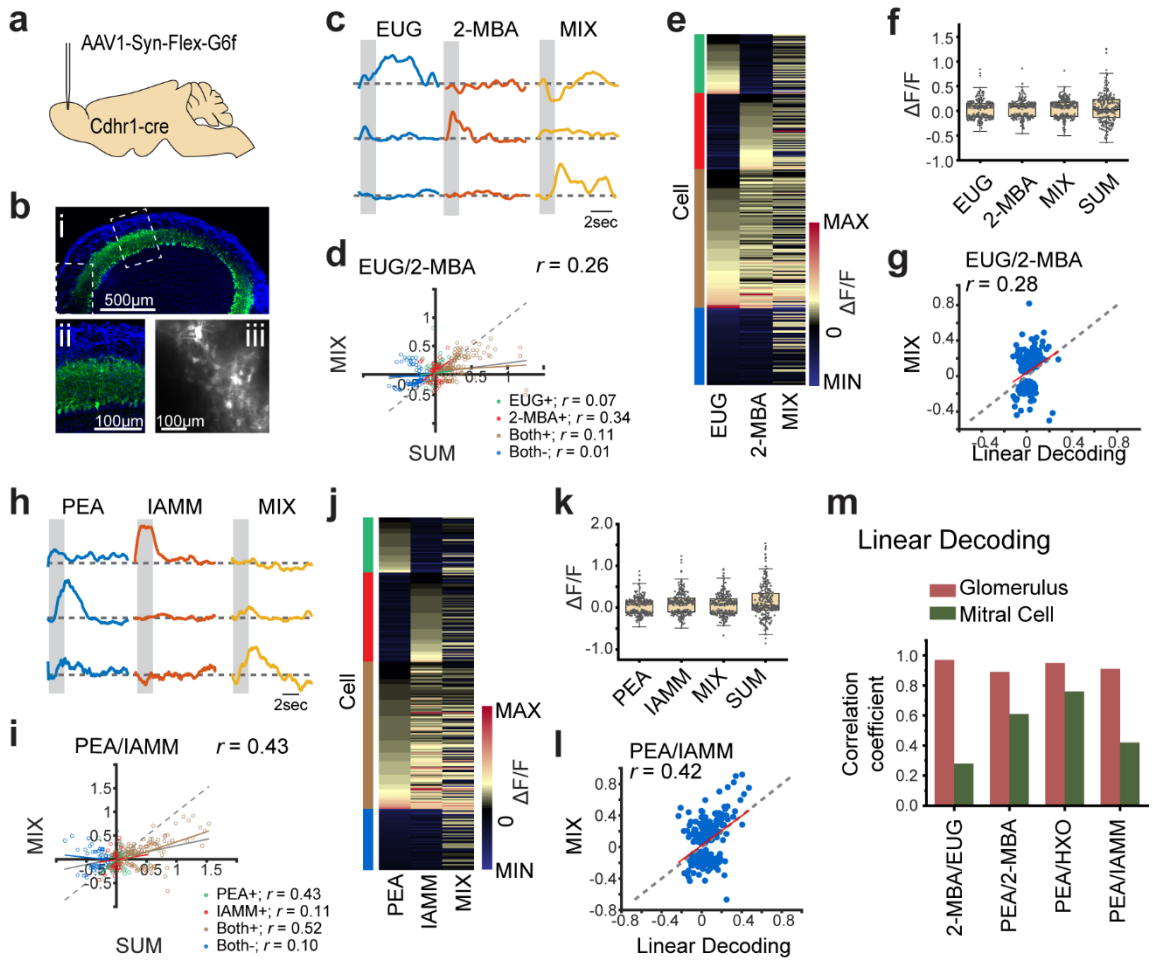

Fig. 3: Cross talk among odor channels in the mitral/tufted cell population

a Illustration of the virus induced mitral cell GCaMP6f expression in mitral cells.

b i, GCaMP6f expression in olfactory bulb after 3 weeks virus expression. ii, higher magnification for the box area in i. iii, a 2-photon image showing the cells under recording condition. Green: GCaMP6f. Blue: DAPI.

c Sample traces of mitral/tufted cell response to eugenol, 2-MBA and their mixture. Each panel is a different cell. Gray box indicates odor delivery period.

d Scatter plot of mitral/tufted cell response amplitude evoked by the congruent mixture against the sum of response amplitudes to individual odors. Colored responses indicated positive response (increased calcium signal) to EUG only (EUG+), 2-MBA only (2-MBA+) or both odors (Both+), and negative response (decrease in calcium signal) to both odors (Both-). Gray line indicates the linear fit of all the data. Colored lines indicate

bioRxiv preprint first posted online Jan. 29, 2020; doi: http://dx.doi.org/10.1101/2020.01.28.923748. The copyright holder for this preprint (which was not peer-reviewed) is the author/funder, who has granted bioRxiv a license to display the preprint in perpetuity. It is made available under a CC-BY-NC-ND 4.0 International license.

linear fit of each group of data. Correlation coefficients (*r*) and diagonal line (grey dot) are indicated.

e Heatmap shows mitral/tufted cell responses to EUG, 2-MBA and their mixture. Responses are sorted according to their response to EUG only, 2-MBA only, both odors and negative response to both odors. Groups are indicated with the colored bars that are matching the colors in **d.**

f Box plot shows the distribution of mitral/tufted cell response amplitude to odors: EUG, 2-MBA, their mixture and the arithmetic sum of component odors. Box plot edges indicate the first and third quartiles of the data, while whiskers indicate 1.5 interquartile range.

g Scatter plot of response of individual mitral/tufted cells to the mixture against the predicted response from linear decoding for odor pair EUG/2-MBA. Red line indicates linear fit of the data. Correlation coefficient (*r*) and diagonal line (grey dot) are indicated.

h-l same as **c-g** but for two aversive odor pair PEA/IAMM.

m Bar graphs shows the correlations coefficients (*r*) between linearly decoded and the actual responses in the glomeruli (wine color) and mitral cells (olive color) for the four odor pairs.

bioRxiv preprint first posted online Jan. 29, 2020; doi: http://dx.doi.org/10.1101/2020.01.28.923748. The copyright holder for this preprint (which was not peer-reviewed) is the author/funder, who has granted bioRxiv a license to display the preprint in perpetuity. It is made available under a CC-BY-NC-ND 4.0 International license.

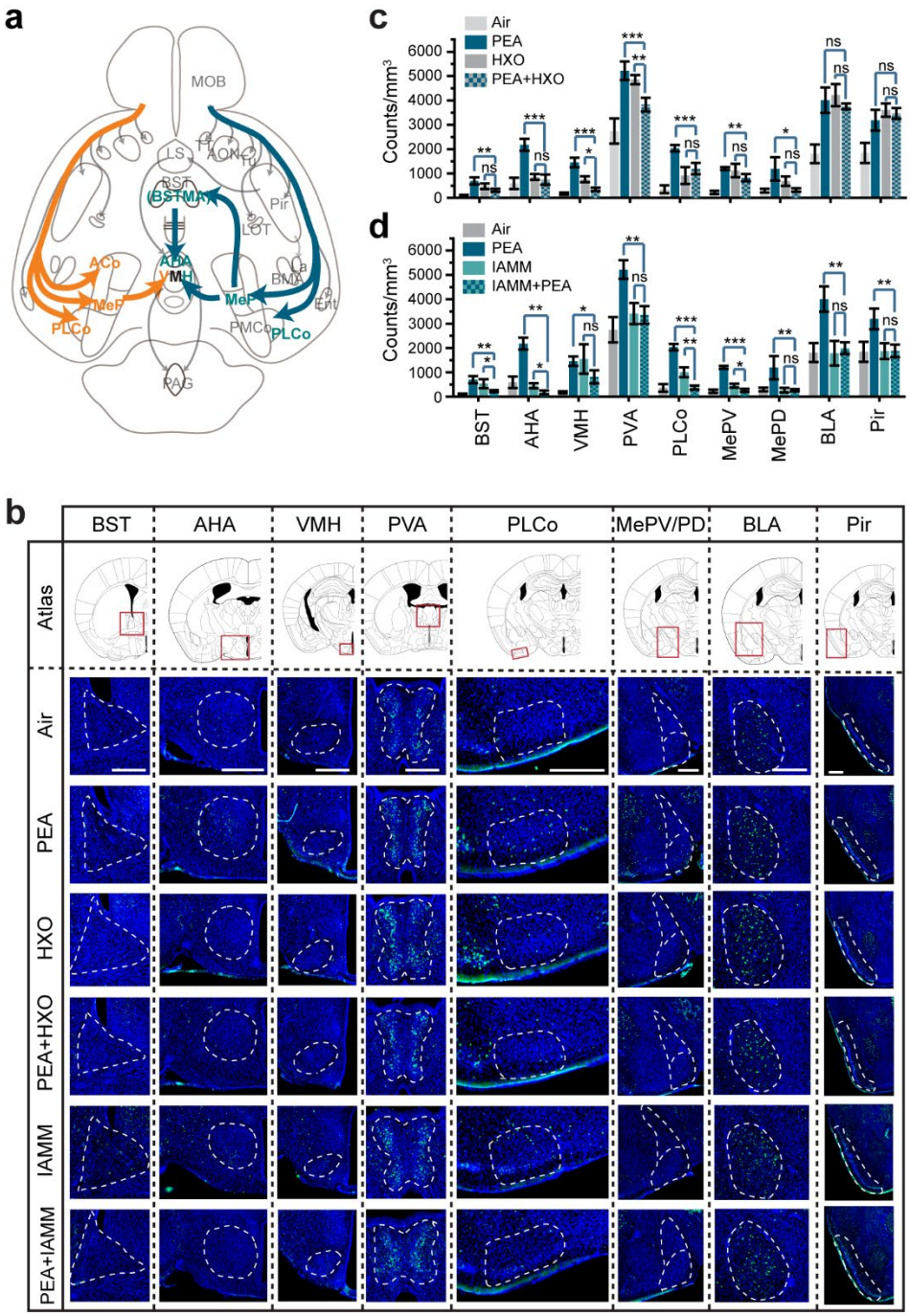

Fig. 4: Altered representation of innate odors in the brain

a Illustration of pathways processing information about innately recognized odors. Pathway and brain areas activated by attractive odors are marked by orange color. Dark olive color labels mark those for innately aversive odors.

bioRxiv preprint first posted online Jan. 29, 2020; doi: http://dx.doi.org/10.1101/2020.01.28.923748. The copyright holder for this preprint (which was not peer-reviewed) is the author/funder, who has granted bioRxiv a license to display the preprint in perpetuity. It is made available under a CC-BY-NC-ND 4.0 International license.

b Immunofluorescent staining of phospho-S6 (green) of brain sections from animals exposed to air, PEA, HXO, PEA+HXO, IAMM and PEA+IAMM. Cell nuclei were counter-stained with DAPI (blue). The areas being quantified are marked by dashed lines. Scale bars, 500 μm.

c Bar plots of the density of activated cells in different brain areas for control, PEA, HXO and their mixture in **b** (data are shown in mean ± SEM, n = 6 half brains).

d Bar plots show the density of activated cells in brain areas for control, PEA, IAMM and their mixture. Data are shown in mean ± SEM, n = 6 half brains.

Abbreviation: AHA: anterior cortical amygdaloid area; AON: anterior olfactory nucleus; BLA: basolateral amygdaloid nucleus, anterior part; BMA: basomedial amygdaloid nucleus, anterior part; BSTMA: bed nucleus of the stria terminalis, medial division, anterior part; Ent: entorhinal cortex; La: lateral amygdaloid nucleus; LOT: lateral olfactory tract; MOB: LS: lateral septal nucleus; main olfactory bulb; MePD: medial amygdaloid nucleus, posterodorsal part; MePV: medial amygdaloid nucleus, posteroventral part; VMH: ventromedial hypothalamic nucleus; PAG: periaqueductal gray; PVA: paraventricular thalamic nucleus, anterior part; Pir: piriform cortex; PLCo: posterolateral cortical amygdaloid area; pmCo: posteromedial cortical amygdaloid nucleus; TT: tenia tecta; Tu: olfactory tubercle.

bioRxiv preprint first posted online Jan. 29, 2020; doi: http://dx.doi.org/10.1101/2020.01.28.923748. The copyright holder for this preprint (which was not peer-reviewed) is the author/funder, who has granted bioRxiv a license to display the preprint in perpetuity. It is made available under a CC-BY-NC-ND 4.0 International license.

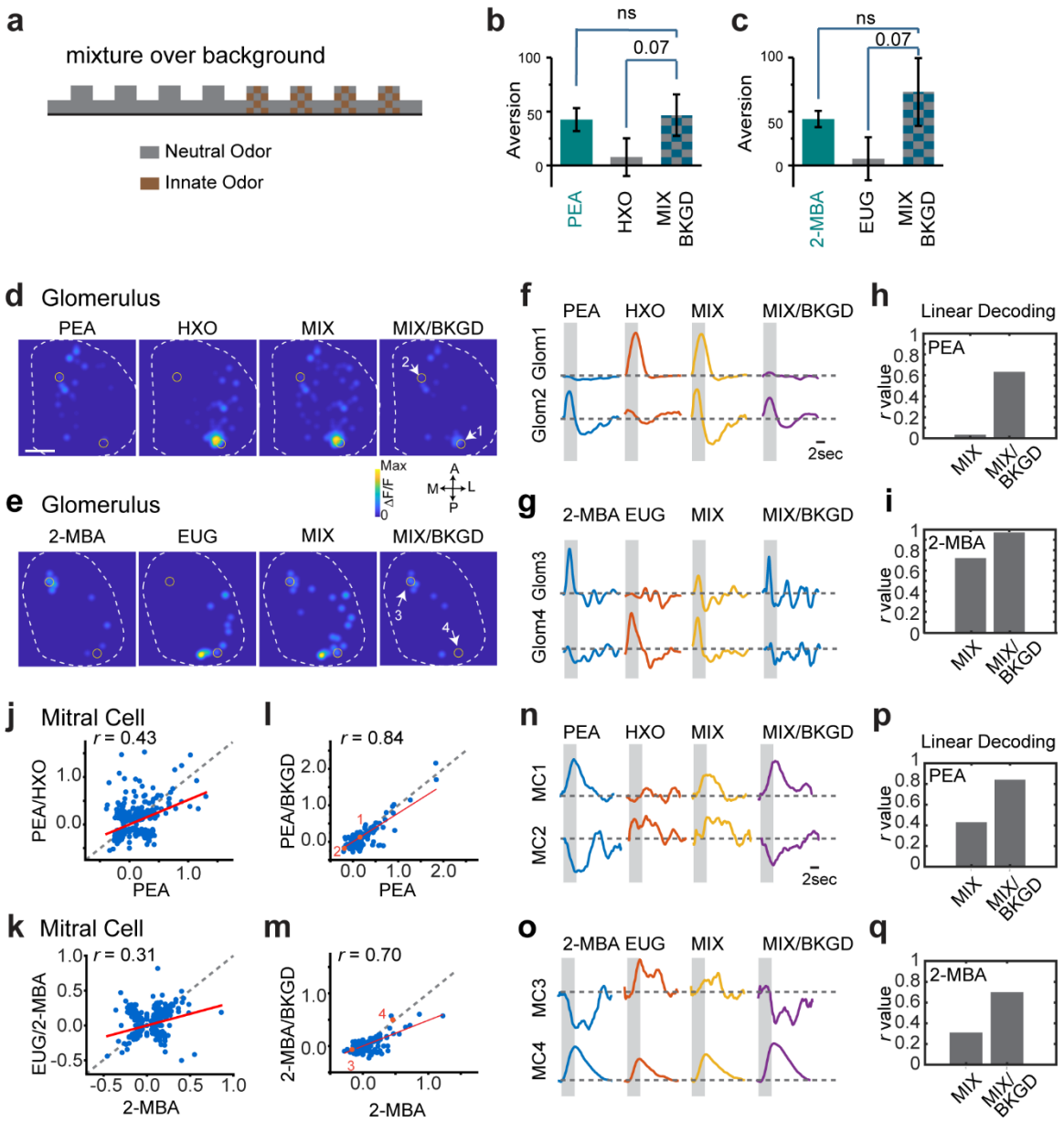

Fig. 5: background presentation allows odor recognition

a Illustration of experimental setup. A neutral odor is continuously delivered whereas the aversive odor is delivered together with the neutral odor during the marked epochs.

b, c Bar plots of aversion measured for PEA, HXO and the mixture (MIX, **b**), and 2-MBA, EUG and their mixture (**c**) when the neutral odors were presented as background.

bioRxiv preprint first posted online Jan. 29, 2020; doi: http://dx.doi.org/10.1101/2020.01.28.923748. The copyright holder for this preprint (which was not peer-reviewed) is the author/funder, who has granted bioRxiv a license to display the preprint in perpetuity. It is made available under a CC-BY-NC-ND 4.0 International license.

d, e Glomerulus activation patterns elicited by PEA/HXO (**d**) or 2-MBA/EUG (**e**) mixture after exposed to HXO (**d**) or EUG (**e**) as background.

f, g Traces of glomerular (Glom, indicated in **d** and **e**) responses to individual odors, their mixture in the absence and presence of background presentation for odor pairs PEA/HXO (**f**) and 2-MBA/EUG (**g**) respectively.

h, i Bar graphs shows the correlations coefficients (*r*) between linearly decoded mixture response and the actual glomerular responses to PEA (**h**) or 2-MBA (**i**) with or without background presentation.

j, k Scatter plots of mitral cell responses to PEA/HXO mixture against that to PEA (**j**), and 2-MBA/EUG against 2-MBA (**k**) without background presentation. Red line indicates linear fit of the data. Correlation coefficient (*r*) and diagonal line (grey dot) are indicated.

l, m Same as **j** and **k** but with the neutral odor presented as background.

n, o Traces of mitral cells (MC, indicated in **l** and **m**) responded to individual odors, their mixture with or without background presentation for odor pairs PEA/HXO (**n**) and 2-MBA/EUG (**o**) respectively.

p, q Bar graphs shows the correlations coefficients (*r*) between linearly decoded mixture response and the actual mitral/tufted cell responses to PEA (**p**) or 2-MBA (**q**) with or without background presentation. Correlation coefficient (*r*) values are plotted.

bioRxiv preprint first posted online Jan. 29, 2020; doi: http://dx.doi.org/10.1101/2020.01.28.923748. The copyright holder for this preprint (which was not peer-reviewed) is the author/funder, who has granted bioRxiv a license to display the preprint in perpetuity. It is made available under a CC-BY-NC-ND 4.0 International license.

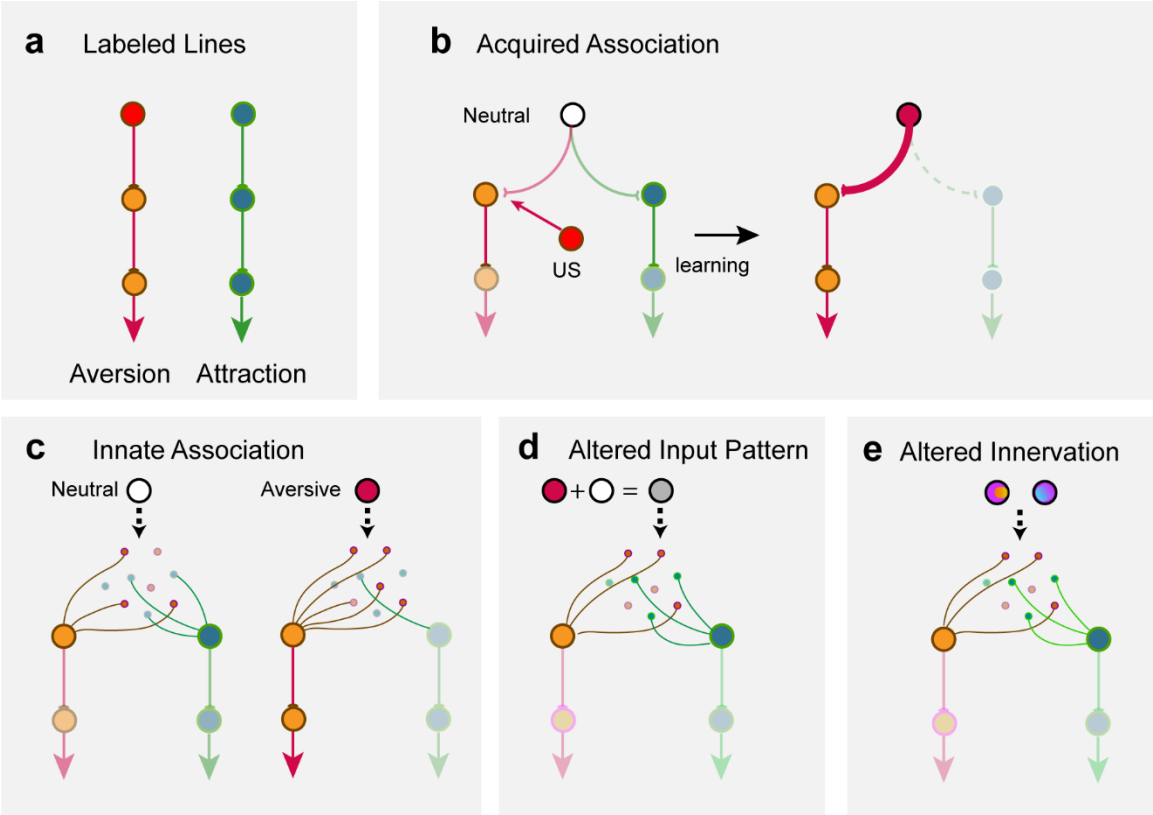

Fig. 6: Models of encoding innate valence of odors

a The labeled-line model. Receptor activations are directly linked to behavioral outputs.

b Acquiring valence through associative learning. A neutral stimulus has an unbiased connection to circuits leaning to attraction or aversion. A teaching signal such as an unconditioned stimulus (US) is associated with the neutral stimulus to enhance its connection to attraction, leading to learned response.

c A model of innate odor preference. Neutral odors (white) activate sets of cells that do not have preferential connection to valence centers. Activation of a specific set of glomeruli (red) activates a set of cells, which encode the odor identity and are stereotypically connected to brain centers that assign valence.

d, e Alterations in the activation of these cells, either through simultaneous activation of additional receptors (**d**) or through ectopic axon projections into multiple glomeruli (**e**), changes the identity of the odor being encoded and leading to changes in valence assignment.